Correlation between the microstructures and the deformation mechanisms of CuZr-based bulk metallic glass composites

K. K. Song, S. Pauly, B. A. Sun, J. Tan, M. Stoica, U. Kühn, and J. Eckert

Citation: AIP Advances **3**, 012116 (2013); doi: 10.1063/1.4789516
View online: https://doi.org/10.1063/1.4789516
View Table of Contents: http://aip.scitation.org/toc/adv/3/1
Published by the American Institute of Physics

Correlation between the microstructures and the deformation mechanisms of CuZr-based bulk metallic glass composites

K. K. Song,[1,2,a] S. Pauly,[1,a] B. A. Sun,[1] J. Tan,[1,2,3] M. Stoica,[1] U. Kühn,[1] and J. Eckert[1,2]

[1]*IFW Dresden, Institut für Komplexe Materialien, Helmholtzstraße 20, D-01069 Dresden, Germany*
[2]*Institut für Werkstoffwissenschaft, TU Dresden, D-01062 Dresden, Germany*
[3]*College of Materials Science and Engineering, Kunming University of Science and Technology, 650093 Kunming, China*

(Received 27 November 2012; accepted 11 January 2013; published online 18 January 2013)

The variation of the transformation-mediated deformation behavior with microstructural changes in CuZr-based bulk metallic glass composites is investigated. With increasing crystalline volume fraction, the deformation mechanism gradually changes from a shear-banding dominated process as evidenced by a chaotic serrated flow behavior, to being governed by a martensitic transformation with a pronounced elastic-plastic stage, resulting in different plastic deformations evolving into a self-organized critical state characterized by the power-law distribution of shear avalanches. This is reflected in the stress-strain curves by a single-to-"double"-to-"triple"-double yielding transition and by different mechanical properties with different serrated flow characteristics, which are interpreted based on the microstructural evolutions and a fundamental energy theorem. Our results can assist in understanding deformation behaviors for high-performance metastable alloys. [http://dx.doi.org/10.1063/1.4789516]

Bulk metallic glasses (BMGs) possess many attractive properties such as high strength and a large elastic limit. However, their use as structural materials is severely limited due to their poor ductility at room temperature arising from shear localization.[1–5] To overcome their intrinsic brittleness, many strategies have been proposed and one effective way is to design bulk metallic glass composites (BMGCs) by *in-situ* or *ex-situ* introduction of the crystalline phase into the glassy matrix.[6–11] So far, various BMGCs containing crystalline phases with different length scales and crystalline volume fractions (f_{cryst}) have been fabricated,[6–11] particularly in the recently developed CuZr-based BMGCs containing metastable B2 phase precipitates.[12–18] Owing to the martensitic transformation (MT) of the metastable B2 phase during deformation at room temperature, stress redistribution in the glassy matrix and transformation-mediated plasticity can be observed.[12–18] As the introduction of ductile phase into the glassy matrix, the formation of multiple shear bands implies that the serrated flow characteristics may be correspondingly changed, which should be further addressed. Then the physical mechanisms determining the yielding and subsequent plastic deformation are yet to be resolved. In this letter, the macroscopic deformation response to the microstructural features in CuZr-based BMGCs was well established.

$Cu_{47.5}Zr_{47.5}Al_5$ BMG and its composites (labeled as BMG, and S1 to S5 in Fig. 1(a)) with different f_{cryst} were fabricated by suction casting using different melting currents/times (i.e. 150 A/10s, 86 mA/15s and 130 mA/10s) or by injection casting varying the melting temperatures.[18]

[a]Author to whom correspondence should be addressed. E-mail: songkaikai8297@gmail.com (K. K. Song); s.pauly@ifw-dresden.de (S. Pauly)

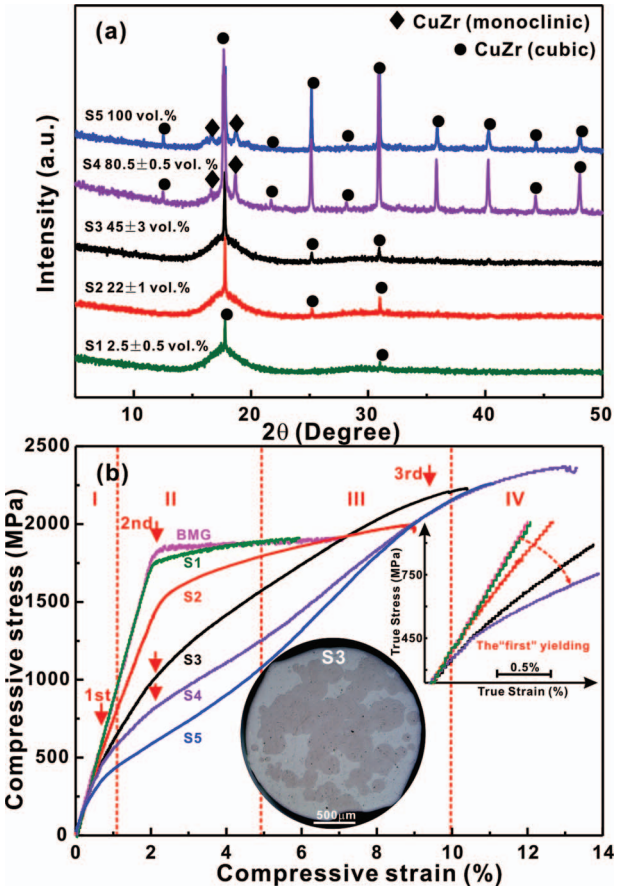

FIG. 1. (a) XRD patterns and (b) the engineering stress-strain curves of the as-cast samples (Insets: OM picture and the magnified "first yielding", respectively; Partial results reprinted from K. K. Song, S. Pauly, Y. Zhang, R. Li, S. Gorantla, N. Narayanan, U. Kühn, T. Gemming, and J. Eckert, Acta Materialia 2012; http://dx.doi.org/10.1016/j.actamat.2012.07.015, Copyright 2012, With permission from Elsevier.).[18]

Compression tests were performed at room temperature using an Instron 5869 testing machine at an initial strain rate of 2.5×10^{-4} s^{-1}. The structures of all the samples were characterized using an X-ray diffractometer (XRD, STOE STADI P, $\lambda = 0.07093187$ nm), a Zeiss Axiophot optical microscope (OM) and a scanning electron microscope (SEM, Gemini 1530). The XRD patterns (Fig. 1(a)) show that sharp Bragg peaks superimpose diffuse diffraction maxima, indicating that the samples consist of amorphous phase and B2 phase and/or martensite. The enhanced crystalline peaks from the S1 to S5 samples implies that f_{cryst} gradually increases,[19] being roughly determined from the area ratio of the amorphous and crystalline phases extracted from OM pictures (middle inset in Fig. 1(b)). When f_{cryst} is larger than 45 ± 3 vol.%, some martensitic crystals (basic structure $P2_{1/m}$ and superstructure Cm) precipitate in the glassy matrix.[12,19] However, the overall deformation behaviors of all the composites are not strongly affected by a minor amount of martensitic crystals due to their limited ductility and strength.[12,18,19]

The compressive stress-strain curves (Fig. 1(b)) for the as-cast samples exhibit different yielding behaviors, significant plastic strains and obvious work hardening. Generally, when a dual-phase composite is subjected to loading, an elastic-elastic stage, a limited elastic-plastic stage and then a plastic stage are experienced in turn.[20] More interesting in Fig. 1(b) is the variation of the yield strengths and the difference in the transition from the elastic to the plastic regime with increasing f_{cryst}. As shown in Fig. 1(b), without any crystals (BMG) or for a very low f_{cryst} (S1, 2.5 ± 0.5 vol.%), a distinct yielding is observed at strains a bit lower than 2%. With gradually increasing f_{cryst} from 22 ± 1 vol.% to 80.5 ± 0.5 vol.%, the yielding behavior of the composites (e.g. S2, S3

and S4) changes and the yield strength becomes more difficult to identify. The elastic-plastic stage becomes clearer, resulting in the formation of a "double yielding" or "triple yielding" behavior, thus dividing the whole deformation into maximum four different stages (Fig. 1(b)). As f_{cryst} reaches up to 22 ± 1 vol.% (S2), a blurry "double yielding" begins to appear. The "first yielding" strain and stress are 0.95 % and 734 MPa while the "second yielding" occurs about 2 % and 1465 MPa, respectively. For f_{cryst} larger than 45 vol.%, a "third yielding" appears (S3 and S4). However, the fully crystalline sample (S5) again only exhibits a double yielding behavior, which, yet, is different than that of the S2 sample.[21]

As illustrated in the right inset in Fig. 1(b), the "first yielding" gradually becomes clearer with increasing f_{cryst}. Fig. 2 displays the variations of the yield strains/stresses as a function of f_{cryst}. The stress range of the elastic-plastic stage (stage II in Fig. 1(b)) is gradually enlarged, but the maximum strain (Fig. 1(c)) is approximately 2 %. It is found that the "first" yield strength of the composites can be modeled by the load-bearing model:[12,22]

$$\sigma_{Composite} = \sigma^{Crystalline}\,(1 + 0.5\,f_{Glass})\,, \tag{1}$$

where f and σ are the volume fractions of the constituent phases and the yield strength, respectively, while the "second yield" strength can be modeled by the rule of mixtures (ROM) model (Fig. 2(b)):[12,23]

$$\sigma_{Composite} = f_{Cryst}\sigma^{Crystalline} + f_{Glass}\sigma^{Glass}. \tag{2}$$

As shown in Fig. 2(b), when f_{cryst} is larger than 22 ± 1 vol.%, the "first yielding" is easily confused with the "second yielding", implying that the crystals start to impinge with each other and a percolation threshold occurs.[12,18] Recently, the percolation theory has been widely used for modeling the deformation behavior of heterogeneous materials.[12,17,24] The percolation threshold occurs in dual-phase composites as the f_{cryst} lies between 10 vol.% and 50 vol.%.[12,24] Hence, the "second yielding" is not pronounced below the percolation threshold, whereas the "first yielding" is inconspicuous above it, resulting in a real yielding percolation transition in CuZr-based BMGCs with increasing f_{cryst}.[12] Generally, the interpenetration of B2 crystals starts at a low f_{cryst} and in the vicinity of 50 vol.% the crystals form a structural framework.[12] In our case, the critical f_{cryst} for the transition is determined to 22 ± 1 vol.%, as sketched by the dash dot line in Fig. 2(b). It is noticed that as f_{cryst} increases from 2.5 ± 0.5 vol.% to 100 vol.%, the fracture strain first increases from 6.1 ± 0.5% to 14.3 ± 0.5% and then decreases to 11.7 ± 0.5% (Fig. 2(a)), and the corresponding fracture strengths also show a similar tendency (Fig. 2(b)). The corresponding fracture strain/stress cannot be described by the ROM and the load-bearing models due to the following possible reasons:[9,12,17,25–31] (i) the macroscopic softening from SBs and the work hardening caused by the MT are not taken into account and (ii) the interactions between SBs and the crystals, and the length-scale of the constituents compared to the characteristic plastic zone size are not sufficiently considered. Based on previous data and our observation for $Cu_{47.5}Zr_{47.5}Al_5$ BMGCs,[12,18] the optimum f_{cryst} with respect to the fracture strength is determined to lie between 40 vol.% and 80 vol.% (inset in Fig. 2(b)), depending on different casting conditions.[12,15,17,30] In the percolation theory, which can well describe the plastic/fracture strains of BMGCs,[12,17] there is a maximum for the plastic/fracture strains for $Cu_{47.5}Zr_{47.5}Al_5$ BMGCs, further confirming our observation.

Based on the macroscopic deformation responses and previous results,[12–18,32–34] the deformation mechanisms of metastable $Cu_{47.5}Zr_{47.5}Al_5$ alloys can be classified into five types: The first constitutes the monolithic BMG whose mechanical properties are strongly affected by the existence of nanoscale crystals in the glassy matrix.[32–34] Significant plastic strain results from the multiplication of SBs induced by nanoscale heterogeneities.[32,34,35] Without nanocrystals in the glassy matrix,[33] the BMG exhibits a limited plasticity (Fig. 1(b)), and the deformation behavior is dominated by one main shear banding process.[32–34] Secondly, for a limited f_{cryst} (S1, 2.5 ± 0.5 vol.%), one yielding is still observed. However, before yielding, martensitic plates are found within some B2 CuZr crystals without any SBs formed in the glassy matrix (Fig. 3(a)). After yielding, multiple SBs are observed (Fig. 3(b)). The third type of deformation is represented by BMGCs with f_{cryst} up to 22 ± 1 vol.%, where the "first yielding" is clearly related to the MT of B2 phase, within which slip bands occur (Fig. 3(c)). After the "second yielding", the martensite volume fraction quickly increases and

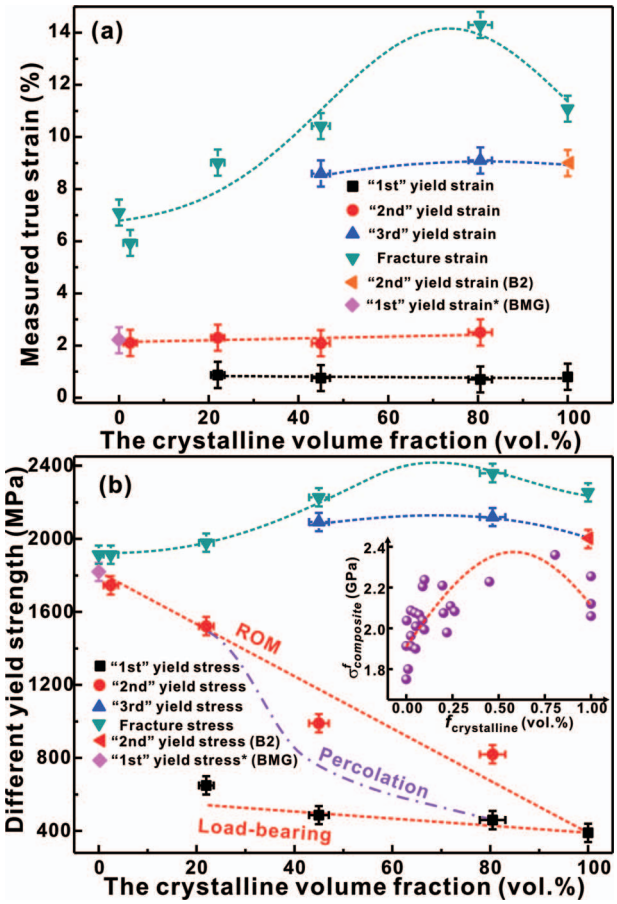

FIG. 2. (a) Different yielding and fracture strains, and (b) different yield strengths and fracture strengths with increasing f_{cryst} (Inset: fracture strengths for different f_{cryst}).

multiple SBs are induced (Fig. 3(d)). Fourthly, when f_{cryst} is higher than 22 ± 1 vol.%, i.e. 45 ± 3 vol.% - 80.5 ± 0.5 vol.%, a "triple yielding" behavior is observed (Fig. 1(b)), possibly due to:[18] (i) the "first yielding" results from the yielding of the B2 phase and the initiation of its MT; (ii) the "second yielding" originates from the further development of MT and the multiplication of SBs; (iii) the "third yielding" is due to the formation of a high density of dislocations and partial detwinning. For the fully crystalline alloy, again a double yielding is observed, which results from the formation of MT and de-twinning/dislocations with a high density.[21] For this fifth type, no rigid glassy matrix is present to provide the constraint, which weakens the effect of de-twinning and dislocations and hence decreases the fracture strength/strain (Fig. 1(b)). Nevertheless, the deformation mechanisms of the metastable CuZr-based alloys with increasing f_{cryst} are gradually dominated from a shear-banding to a MT, leading to a single-to-"double"-to-"triple"-to-double yielding transition.

From a thermodynamic point of view, the dynamic instability of SBs and the plastic deformation of metallic glasses can be evaluated by a shear-band instability index, λ_{crit}:[36]

$$\lambda_{crit} = L\left(1 + \frac{\pi d^2}{4LK_M}E_y\right), \tag{3}$$

where L, d, and E_y are the height, the diameter, the stiffness and the Young's modulus of the sample, respectively, while K_M is the machine stiffness. The effective Young's modulus of the dual-phase

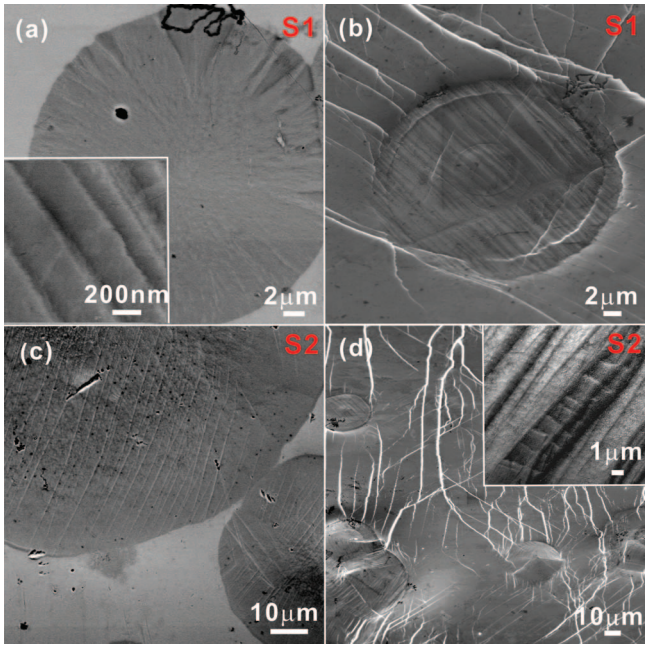

FIG. 3. Surface morphology of (a-b) the S1 sample and (c-d) the S2 sample after the "first yielding" and the "second yielding", respectively (Insets in (a) and (d): twinned martensitic plates).

composite can be obtained:[37]

$$E_{composite} = E_{matrix}\left[1 + \frac{f_{cryst}\left(E_{cryst} - E_{matrix}\right)}{\left(1 - f_{cryst}\right)\beta\left(E_{cryst} - E_{matrix}\right) + E_{matrix}}\right], \quad (4)$$

where E_{matrix} and E_{cryst} are Young's modulus of the amorphous and ductile phase, respectively, β is calculated by $\beta = 2(4\text{-}5\nu_{matrix})/15(1\text{-}\nu_{matrix})$, and ν_{matrix} is the Poisson ratio of the matrix.[37] Based on the Eq. (4) and precious results,[12] the E of the composite can be estimated to decrease from 89 ± 2 GPa to 82 ± 2 GPa with an increasing crystalline volume fraction. Then the calculated λ_{crit} of CuZr-based BMGCs gradually decreases from 7.8 mm with increasing f_{cryst}. Besides, the ductile phase in the glassy matrix may serve as heterogeneous nucleation site for the initiation of SBs and act as pinning centers during SB propagation during plastic deformation.[6–9] Then for the ductile-phase reinforced CuZr-based BMGCs, shear banding gradually progresses in a more stable way.[36] Therefore, with increasing f_{cryst}, the mean free path of the SBs is reduced and the shear offset generated by each shear event is reduced. Generally, the movement of the SBs in metallic glasses is directly related with the activation of shear transformation zones (STZs), and their dynamics is reflected by serrations in the respective stress-strain curves.[38–41] For the $Cu_{47.5}Zr_{47.5}Al_5$ BMG without obvious nanocrystals,[33] the serrated flow is observed and its statistics the number of stress drops $N(\Delta\sigma_s)$ with a given stress amplitude are counted. The corresponding histogram displays a relatively broad distribution described by a Gaussian distribution (Fig. 4(a)), implying a chaotic behavior.[38,42] For the $Cu_{47.5}Zr_{47.5}Al_5$ BMG containing nanocrystals,[32,38] the stress drop distribution follows a power-law with an exponent, $\alpha = 1.49$, indicating a self-organized intermittent plastic flow behavior.[38,43,44] As the B2 phase is introduced into the glassy matrix, the S1 sample also exhibits numerous flow serrations (Fig. 4(b)) and the serrated flow also evolves into a self-organized state with a power-law exponent of 1.25. Therefore, the dynamics of the serrated flow of the metastable CuZr-based alloys change from a chaotic state to a self-organized criticality due to the microstructural heterogeneities. However, for the S2 sample, the serrated flow behavior is not obvious but can still be found (Fig. 4(c)). Its α exponent, which is larger than 2, does not fall into the experimental range of 1.3-1.5 for BMGs,[38,43] implying that the MT starts to compete with the shear banding during deformation. As f_{cryst} increases up to 80.5 ± 0.5 vol.%, the enlarged view of the stable plastic stage

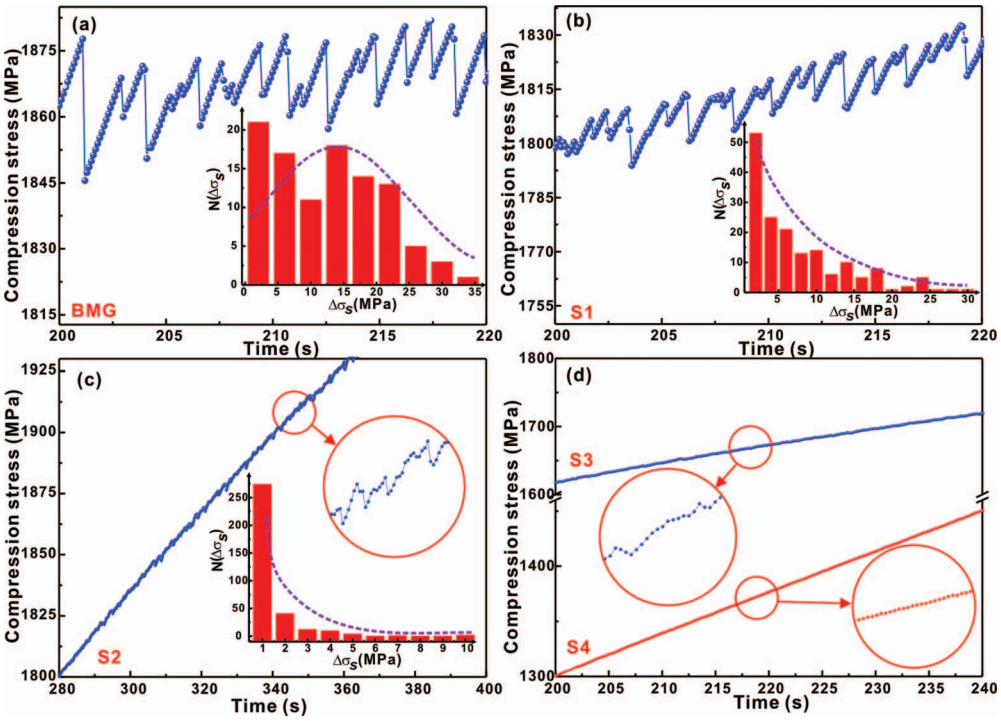

FIG. 4. (a-d) The serrated flows *vs.* the time of the BMG and the S1-S4 samples (Insets: N($\Delta\sigma_s$) vs. the time and magnified serrated flow behavior, with schematic purple curves obtained by Gaussian and power law fits, respectively, whose calculation procedures have been given in Refs. 38 and 42).

(Fig. 4(d)) shows that the number and the magnitude of the stress drops gradually become more and smaller, respectively, so the time - stress curves for the S3 and S4 samples are smoother. Moreover, the S5 crystalline sample does not exhibit any flow serrations, indicating that the deformation is totally dominated by the MT.

Nevertheless, the plastic deformation of metastable CuZr-based alloys is indeed related with the shear banding and MT processes. As proven above, with different scaled microstructural inhomogeneities introducing into a glassy matrix, the shear banding process reflected by different serration behaviors has shown a transition from a chaotic serrated flow behavior represented by a Gaussian distribution of shear avalanches to a self-organized critical state characterized by a power-law distribution of shear avalanches. However, with further increasing f_{cryst}, the plastic process would be dominated by the MT process gradually. As we know, MT, being induced by thermal or deformation factors, is diffusionless structural transformation from a high-temperature crystalline phase to a low-temperature crystalline phase involving a rearrangement of atoms that shears the unit cell.[45–47] As the transformation proceeds by the movement of the habit plane, the new phase forms which would result in large coherency strains in the lattice and the accumulation of the elastic energy.[45–47] The dynamics process of the MT has been investigated by using transient thermal spikes, acoustic emissions, electrical resistivity, conventional x-ray, neutron scattering, and coherent x-ray scattering at third-generation synchrotron sources measurements, respectively,[46–51] which give an indirect or/and direct access to the underlying local dynamics of the MT. It was found that the dynamics of the MT also self-organize into a critical state, which leads to the relief of strain through a series of discrete avalanches,[46,47] i.e. the dissipation of the elastic energy stored during the transformation. The corresponding power-law exponent was found to be larger than that of the dynamics process of shear banding, and increases to 2.8-3.2 in Cu-based shape memory alloys.[46] However, the serrations in the compression curves start to disspear with increasing f_{cryst}, which suggests the scale of the local dynamics of the plastic deformation gradually decreases with the addition of an amount of shape memory B2 CuZr phase into the glassy matrix. Based on fundamental energy theorems, a quasi phase

transition model of SBs in MGs was proposed by analyzing energy changes during shear banding in a sample-machine system.[52] Generally, one serration event related with shear banding consists of an elastic energy accumulation followed by the release of elastic energy. The elastic energy density of one serration event, $\Delta\delta$, can be calculated by $\Delta\delta = \Delta\sigma\,\Delta\varepsilon/2$, where $\Delta\sigma$ and $\Delta\varepsilon$ are the elastic stress and strain in one serration event, respectively.[53] As the SBs start to propagate, the elastic energy of the serration events is consumed by the initiation and propagation of SBs in the local plastic region, i.e. configurational hopping of STZs.[39,43] Then the elastic energy is stored in a sample - testing machine system and is mainly consumed by the initiation and propagation of SBs during deformation.[36] After shear banding, the elastic energy stored ($|\Delta G_E|$) consists of the increase in the volume free energy and the newly generated interfacial free energy, or/and the dissipated energy in the form of heat within the SBs.[52,54] In our case, the formation of phase transformation can also store and dissipate parts of $|\Delta G_E|$, consuming energy in the form of heat and the newly-generated interfacial free energy and so on.[55,56] In fact, the MT is quite pronounced before the formation of SBs especially with increasing f_{cryst}. Thus, the dissipated energy results in a decrease of the elastic energy density of serration events and then slows down the shear-banding process. On the other hand, the SBs can be initiated easily at the interface between the glassy matrix and the crystals due to the high interfacial energy and large stress concentrations at the interface.[6,57] According to the conservation of energy, the SBs may operate more easily but less elastic energy will be dissipated in each shear banding event, facilitating the formation of multiple SBs and impeding their rapid propagation, being reflected from the serrated flow behaviors. Therefore, the number and stress oscillations of the serration events become higher and smaller with increasing f_{cryst}, respectively, confirming the gradual change of the deformation mechanisms.

To conclude, the different yielding and plastic behaviors of the metastable CuZr-based alloys with increasing f_{cryst} results from the MT, and/or the formation of multiple SBs, and/or partial detwinning together with a high density of dislocations, leading to a single-to-"double"-to-"triple"-to-double" yielding transition. The critical f_{cryst} for the transition can be estimated to be 22 vol.% and the optimum f_{cryst} for good mechanical properties lies between 40 - 80 vol.%. The "first" and "second" yield strength can be modeled by the load-bearing model and the ROM, respectively. With increasing f_{cryst}, the elastic energy stored in the system was redistributed, resulting in different serrated flow characteristics and different plastic deformations evolving into a self-organized critical state characterized by the power-law distribution of shear avalanches.

ACKNOWLEDGMENTS

This work was supported by the Chinese Council Scholarship Fund, the National Basic Research Program of China (973 Program 2007CB613901), the National Natural Science Foundation of China (50631010 and 50831003), the Natural Science Foundation of Shandong province (Z2008F08), the Excellent Youth Project of the Natural Science Foundation of Shandong Province (JQ201012) and the German Science Foundation under the Leibniz Program (grant EC 111/26-1). The authors are grateful to B. Bartusch, B. Opitz, D. Lohse, J. Thomas, L. B. Bruno, M. Frey, M. Stoica, S. Donath, U. Wilke and other colleagues at IFW Dresden for technical assistance and stimulating discussions.

[1] H. Chen, Y. He, G. J. Shiflet, and S. J. Poon, Nature **367**, 541 (1994).
[2] W. L. Johnson, MRS Bull. **24**, 42 (1999).
[3] A. Inoue, Acta Mater. **48**, 279 (2000).
[4] Y. H. Liu, G. Wang, R. J. Wang, D. Q. Zhao, M. X. Pan, and W. H. Wang, Science **315**, 1385 (2007).
[5] A. R. Yavari, J. J. Lewandowski, and J. Eckert, MRS Bull. **32**, 635 (2007).
[6] C. C. Hays, C. P. Kim, and W. L. Johnson, Phys. Rev. Lett. **84**, 2901 (2000).
[7] X. Hui, W. Dong, G. L. Chen, and K. F. Yao, Acta Mater. **55**, 907 (2007).
[8] Y. Li, S. J. Poon, G. J. Shiflet, J. Xu, D. H. Kim, and J. F. Loffler, MRS Bull. **32**, 624 (2007).
[9] D. C. Hofmann, J. Y. Suh, A. Wiest, G. Duan, M. L. Lind, M. D. Demetriou, and W. L. Johnson, Nature **451**, 1085 (2008).
[10] C. P. Kim, Y. S. Oh, S. Lee, and N. J. Kim, Scripta Mater. **65**, 304 (2011).
[11] J. W. Qiao, A. C. Sun, E. W. Huang, Y. Zhang, P. K. Liaw, and C. P. Chuang, Acta Mater. **59**, 4126 (2011).
[12] S. Pauly, G. Liu, G. Wang, U. Kühn, N. Mattern, and J. Eckert, Acta Mater. **57**, 5445 (2009).
[13] D. C. Hofmann, Science **329**, 1294 (2010).
[14] Y. Wu, Y. Xiao, G. Chen, C. T. Liu, and Z. Lu, Adv. Mater. **22**, 2770 (2010).

[15] K. K. Song, S. Pauly, Y. Zhang, P. Gargarella, R. Li, N. S. Barekar, U. Kühn, M. Stoica, and J. Eckert, Acta Mater. **59**, 6620 (2011).
[16] Y. Wu, H. Wang, H. H. Wu, Z. Y. Zhang, X. D. Hui, G. L. Chen, D. Ma, X. L. Wang, and Z. P. Lu, Acta Mater. **59**, 2928 (2011).
[17] Z. Liu, R. Li, G. Liu, W. Su, H. Wang, Y. Li, M. Shi, X. Luo, G. Wu, and T. Zhang, Acta Mater. **60**, 3128 (2012).
[18] K. K. Song, S. Pauly, Y. Zhang, R. Li, S. Gorantla, N. Narayanan, U. Kühn, T. Gemming, and J. Eckert, Acta Mater. **In Press**, http://dx.doi.org/10.1016/j.actamat.2012.07.015.
[19] S. Pauly, J. Das, J. Bednarcik, N. Mattern, K. B. Kim, D. H. Kim, and J. Eckert, Scripta Mater. **60**, 431 (2009).
[20] S. H. Xia and J. T. Wang, Int. J. Plast. **26**, 1442 (2010).
[21] S. Pauly, J. Bednarčik, U. Kühn, and J. Eckert, Scripta Mater. **63**, 336 (2010).
[22] N. Ramakrishnan, Acta Mater. **44**, 69 (1996).
[23] U. Hangen and D. Raabe, Acta Metall. Mater. **43**, 4075 (1995).
[24] C. W. Nan, Prog Mater. Sci. **37**, 1–116 (1993).
[25] Z. Fan and A. P. Miodownik, Scripta Metall. Mater. **28**, 895 (1993).
[26] M. F. Ashby and A. L. Greer, Scripta Mater. **54**, 321 (2006).
[27] S. F. Corbin and D. S. Wilkinson, Acta Metall. Mater. **42**, 1311 (1994).
[28] Z. Li, S. Schmauder, and M. Dong, Comp. Mater. Sci. **15**, 11 (1999).
[29] K. K. Song, S. Pauly, B. A. Sun, Y. Zhang, J. Tan, U. Kühn, M. Stoica, and J. Eckert, Intermetallics **30**, 132 (2012).
[30] H. Choi-Yim, R. D. Conner, F. Szuecs, and W. L. Johnson, Acta Mater. **50**, 2737 (2002).
[31] S. Pauly, G. Liu, S. Gorantla, G. Wang, U. Kühn, D. H. Kim, J. Eckert, Acta Mater. **58**, 4883 (2010).
[32] J. Das, M. B. Tang, K. B. Kim, R. Theissmann, F. Baier, W. H. Wang, and J. Eckert, Phys. Rev. Lett. **94**, 205501 (2005).
[33] Q. P. Cao, J. F. Li, Y. H. Zhou, and J. Z. Jiang, Scripta Mater. **59**, 673 (2008).
[34] S. Pauly, S. Gorantla, G. Wang, U. Kühn, and J. Eckert, Nature Mater. **9**, 473 (2010).
[35] A. Inoue, W. Zhang, T. Tsurui, A. R. Yavari, and A. L. Greer, Phil. Mag. Lett. **85**, 221 (2005).
[36] Y. Q. Cheng, Z. Han, Y. Li, and E. Ma, Phys. Rev. B **80**, 134115 (2009).
[37] Z. Hashin and S. Shtrikman, J. Mech. Phys. Solids **11**, 127 (1963).
[38] B. A. Sun, H. B. Yu, W. Jiao, H. Y. Bai, D. Q. Zhao, and W. H. Wang, Phys. Rev. Lett. **105**, 035501 (2010).
[39] G. Wang, K. C. Chan, L. Xia, P. Yu, J. Shen, and W. H. Wang, Acta Mater. **57**, 6146 (2009).
[40] W. L. Johnson, M. D. Demetriou, J. S. Harmon, M. L. Lind, and K. Samwer, MRS Bull. **32**, 644 (2007).
[41] J. J. Lewandowski and A. L. Greer, Nature Mater. **5**, 15 (2006).
[42] J. W. Qiao, Y. Zhang, and P. K. Liaw, Intermetallics **18**, 2057 (2010).
[43] R. Sarmah, G. Ananthakrishna, B. A. Sun, and W. H. Wang, Acta Mater. **59**, 4482 (2011).
[44] M. A. Lebyodkin, Y. Brechet, Y. Estrin, and L. P. Kubin, Phys. Rev. Lett. **74**, 4758 (1995).
[45] K. Otsuka, C. M. Wayman, *Shape memory materials* (Cambridge University Press, Cambridge, 1998).
[46] C. Sanborn and K. F. Ludwig, Phys. Rev. Lett. **107**, 015702 (2011).
[47] E. Vives, J. Ortín, L. Mañosa, I. Ràfols, R. Pérez-Magrané, and A. Planes, Phys. Rev. Lett. **72**, 1694 (1994).
[48] L. Carrillo and J. Ortín, Phys. Rev. B **56**, 11508 (1997).
[49] M. C. Gallardo, J. Manchado, F. J. Romero, J. del Cerro, E. K. H. Salje, A. Planes, E. Vives, R. Romero, and M. Stipcich, Phys. Rev. B **81**, 174102 (2010).
[50] F. J. Pérez-Reche, E. Vives, L. Mañosa, and A. Planes, Phys. Rev. Lett. **87**, 195701 (2001).
[51] U. Chandni, A. Ghosh, H. S. Vijaya, and S. Mohan, Phys. Rev. Lett. **102**, 025701 (2009).
[52] Z. Liu, R. Li, G. Wang, S. Wu, X. Lu, and T. Zhang, Acta Mater. **59**, 7416 (2011).
[53] X. F. Pan, H. Zhang, Z. F. Zhang, M. Stoica, G. He, and J. Eckert, J Mater. Res. **20**, 2632 (2005).
[54] F. H. Dalla Torre, A. Dubach, J. Schällibaum, and J. F. Löffler, Acta Mater. **56**, 4635 (2008).
[55] K. Otsuka and C. M. Wayman, *Shape Memory Materials* (Cambridge University Press, Cambridge, 1998).
[56] M. Ahlers, R. Pascual, R. Rapacioli, and W. Arneodo, Mater. Sci. Eng. **27**, 49 (1977).
[57] Q. S. Zhang, W. Zhang, G. Q. Xie, and A. Inoue, Mater. Trans. **48**, 2542 (2007).